ETH
Eidgenössische Technische Hochschule Zürich
Swiss Federal Institute of Technology Zurich

PHYSICS LABORATORY COURSE
FOR ADVANCED STUDENTS

ALPHAABSORPTION

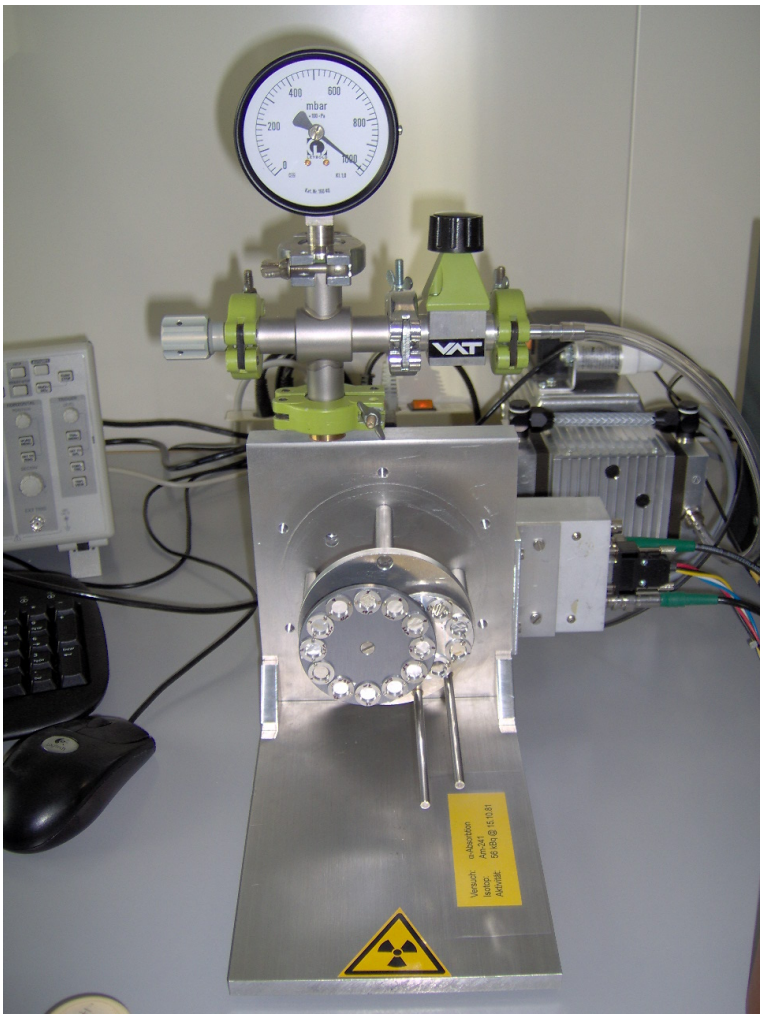

Author : Lukas Wacker, Julián Cancino, Reto Küng, Caroline Haug

April 2009, mod. November 2013, ref. September 2022

Contents

Introduction

When charged particles (here α-particles) pass through matter, they interact with the electrons and the nuclei of the target atoms (Coulomb interaction). The particles lose energy in many steps, until their energy is (almost) zero and are deflected from their primary direction. The following interactions with the target atoms are responsible for this:

1. Inelastic collisions with the target electrons
2. Elastic collisions of the nuclei (Rutherford-scattering)

Process (1) leads to excitation or ionization of the target atoms (electron energy loss), while process (2) (nuclear energy loss) displaces the target atoms (radiation damage) and changes the direction of the charged particle. The mean energy loss per path length (specific energy loss or stopping power) increases with decreasing kinetic energy of the projectile, reaches a maximum and decreases strongly towards the end of the stopping range (Bragg curve). The stopping range depends on the type of particle, on its initial energy and on the material through which it passes.

The nuclear energy loss only becomes significant below 1 MeV/nucleon (when $m_T \gg m_e$) and increases with decreasing kinetic energy. Therefore the probability that a change in direction occurs also increases. The statistical character of the inelastic and elastic collisions is responsible for an energy straggling and an angular straggling of the penetrating particles.

1 Acquisition of knowledge

The following topics shall be understood at the end of the experiment:

1.1 Kinematic of the α-decay

Energy and momentum preservation, excitation energy, determination of the energy of the α-particles, probability of decay.

1.2 Interaction of charged particles with matter

Specific energy loss, Bethe-Bloch-Formula, stopping range, energy straggling

1.3 Principal of a semi-conductor detector

band model of semiconductors, pn-transition, formation of a signal, energy resolution

1.4 Electronics (signal processing)

pre-amplifier, amplifier, analysis of energy spectra

2 Basics

2.1 Specific energy loss (Theory)

In 1913, Niels Bohr derived a classical model [Boh13] for the specific energy loss of charged particles in matter. Despite some strong simplifications this derivation shows the main physical principles. We will therefore briefly follow the derivation step-by-step to understand the processes of energy loss better.

We consider a charged particle 1 with mass m_1, charge $Z_1 e$ (e: elemental charge), that travels with a velocity of v in the x-direction passing by a stationary particle 2 with mass m_2, charge $Z_2 e$ over a distance b (b: collision parameter, see figure 1). We assume, that particle 2 is not noticeably moved when particle 1 passes and will calculate the transition of momentum and energy to particle 2.

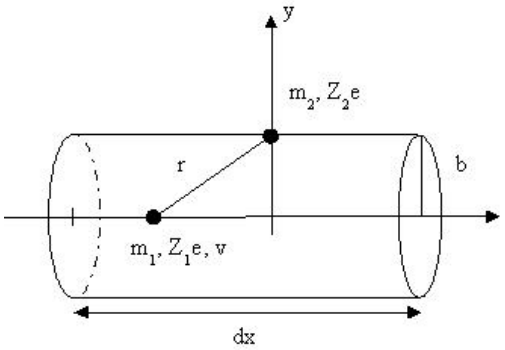

Figure 1: Geometrical representation of the collision process of 2 particles: particle 1 (mass m_1, charge $Z_1 e$, velocity v) passes by a stationary particle 2 (mass m_2, charge $Z_2 e$) within a distance b (impact parameter).

The change in momentum in the x-direction disappears:

$$\Delta p_x = -Z_1 e \int_{-\infty}^{\infty} F_x dt = 0 \tag{2.1}$$

because particle 1 will transfer as much momentum in the positive x-direction as in the negative x-direction.

For the y-direction:

$$\Delta p_y = Z_1 e \int_{-\infty}^{\infty} F_y dt = Z_1 e \int_{-\infty}^{\infty} F_y \frac{1}{v} dx \approx \frac{Z_1 e}{2\pi b v} \int_{-\infty}^{\infty} 2\pi b F_y dx \approx \frac{Z_1 e}{2\pi b v} \frac{Q}{\varepsilon_0} \tag{2.2}$$

The last expression is derived from the divergence theorem (Gauss' theorem), which is a result that relates the flow (that is, flux) of a vector field through a surface to the behavior of the vector field inside the surface.

For the interaction of an individual charge, we have $Q = Q_2 = Z_2 e$ and thus ($\epsilon^2 := \frac{e^2}{4\pi\varepsilon_0} = 1.44[eV \cdot nm]$):

$$\Delta p_{y,2} = \frac{2 Z_1 Z_2}{b v} \epsilon^2 \tag{2.3}$$

We then obtain the transferred energy T from particle 1 (with the energy $E = m_1 v^2/2$) to particle 2:

$$T = \frac{(\Delta p_{y,2})2}{2m_2} = \frac{2Z_1^2 Z_2^2 \epsilon^4}{b^2 v^2 m_2} = \frac{Z_1^2 Z_2^2 \epsilon^4}{b^2 E} \frac{m_1}{m_2} \propto \frac{1}{Eb^2} \tag{2.4}$$

Particle 1 has an energy of $E - T$ after the collision. All particles with the same energy E passing by with the same impact parameter b lose the same energy T.

Now we consider the interaction of a large number of particles in a medium with an atomic density of N particles per unit volume and an atomic number Z. Therefore in this medium we have N atomic nuclei and $n = NZ$ electrons per unit volume, respectively. The total charge per unit volume (charge density) is the same for both the nuclei and the electrons, and equals $Q_2/V = NZe$.

The differential cross section, $d\sigma(T)$, for an energy transfer between T and $T + dT$ is:

$$d\sigma(T) = -2\pi b db \tag{2.5}$$

To include the interaction of all charge carriers, we integrate over differential hollow cylinders with a wall thickness db and a length dx between b_{min} and b_{max}. An integration between 0 and ∞ is meaningless because $b \to 0$ would mean $\Delta E \to \infty$ and $b \to \infty$ would disregard any shielding effects.

For a mean energy loss dE of particle 1 over a distance dx, we therefore obtain the following expression:

$$-\frac{dE}{dx} = n \int_{T_{min}}^{T_{max}} T d\sigma \tag{2.6}$$

In terms of impact factor b we get:

$$-\frac{dE}{dx} = n \int_{b_{max}}^{b_{min}} T 2\pi b db = n \int_{b_{max}}^{b_{min}} \frac{Z_1^2 Z_2^2 \epsilon^4}{b^2 E} \frac{m_1}{m_2} 2\pi b db \tag{2.7}$$

and therefore:

$$-\frac{dE}{dx} = \frac{2\pi n Z_1^2 Z_2^2 \epsilon^4}{E} \frac{m_1}{m_2} \int_{b_{max}}^{b_{min}} \frac{1}{b} db = \frac{2\pi n Z_1^2 Z_2^2 \epsilon^4}{E} \frac{m_1}{m_2} \ln\left(\frac{b_{max}}{b_{min}}\right)) \tag{2.8}$$

We now consider the two quantities b_{min} und b_{max}.

The maximal transfer of energy T_{max} in a single elastic collision between two particles is:

$$T_{max} = \frac{4 m_1 m_2}{(m_1 + m_2)^2} E = \frac{Z_1^2 Z_2^2 \epsilon^4}{b_{min}^2 E} \frac{m_1}{m_2} \tag{2.9}$$

and therefore:

$$b_{min} = \frac{Z_1 Z_2 \epsilon^2}{2E} \frac{m_1 + m_2}{m_2} \tag{2.10}$$

In order to estimate the value of b_{max}, we assume that the corresponding minimal transferred energy ΔE_{min} must be large enough to lift an electron to a higher energy level. We set $\Delta E_{min} = I$, where I is the mean ionization energy of the corresponding atom. In case of an interaction with the target atoms (nuclear energy loss), I corresponds to the mean energy required for a displacement of a target atom.

We therefore obtain:

$$b_{max} = Z_1 Z_2 \epsilon^2 \sqrt{\frac{m_1}{m_2 I E}} \tag{2.11}$$

and therefore:

$$\frac{b_{max}}{b_{min}} = \sqrt{\frac{4 E m_1 m_2}{I(m_1 + m_2)^2}} \tag{2.12}$$

For the mean specific energy loss we therefore obtain:

$$-\frac{dE}{dx} = \frac{2\pi n Z_1^2 Z_2^2 \epsilon^4}{E} \frac{m_1}{m_2} \ln\left(\frac{4 E m_1 m_2}{I(m_1 + m_2)^2}\right) \tag{2.13}$$

This calculation is based on direct collisions with electrons in the solid. There is an other term of comparable magnitude due to distant resonant energy transfer (the derivation is outside the scope of this simple approach). A correct quantum mechanical derivation of the specific energy loss results in a doubled value and an additional term in the logarithm that accounts for the relativistic effects at higher energies and corrections for inner electron shells of the atoms.

With a quantum mechanical, but still without relativistic correction term we therefore obtain ($E = m_1 v^2/2$) :

$$-\frac{dE}{dx} = \frac{4\pi n Z_1^2 Z_2^2 \epsilon^4}{m_2 v^2} \ln\left(\frac{2 m_2 v^2}{I(1 + m_2/m_1)^2}\right) \tag{2.14}$$

Electron energy loss For the electron energy loss ($m_2 = m_e = m \ll m_1$, $Z_2 = 1$, $n = N_e = N_{Atom} Z$) we obtain:

$$-\left.\frac{dE}{dx}\right|_e = \frac{4\pi N_e Z_1^2 \epsilon^4}{m v^2} \ln\frac{2 m v^2}{I} = \frac{4\pi Z_1^2 \epsilon^4}{m v^2} N_{Atom} Z \ln\left(\frac{2 m v^2}{I}\right) \tag{2.15}$$

Nuclear energy loss For a simple estimation, we consider protons with mass $m_p = 1836 * m_e$ as particles fall in.

Without considering the logarithmic term, we obtain the following expression for the ratio of the nuclear to electron energy loss:

$$\frac{-dE/dx|_n}{-dE/dx|_e} = Z_2 \frac{m_e}{m_2} \simeq Z_2 \frac{m_e}{2 Z_2 m_p} \simeq \frac{1}{3600} \tag{2.16}$$

Thereby we have assumed that the target nucleus contains as many protons as neutrons with approximately the same mass: $m_2 \approx 2 Z_2 m_p$.

Already this simple estimation shows that the nuclear energy loss must be significantly smaller than the electron energy loss.

2.2 Specific energy loss (Bethe-Bloch Formula)

Bethe and Bloch derived a formula for the electron energy loss dE per unit length with a correct quantum mechanical calculation (Bethe-Bloch formula). It can be written in the non-relativistic approximation in the following form:

$$-\frac{dE}{dx} = \frac{2\pi z^2 \epsilon^4}{E_T} \frac{m_T}{m_e} N_e \ln\left(\frac{4E_T m_e}{I m_T} - K\right) \tag{2.17}$$

or:

$$\sigma = -\frac{1}{N}\frac{dE}{dx} = \frac{2\pi z^2 \epsilon^4}{E_T} \frac{m_T}{m_e} Z \ln\left(\frac{4E_T m_e}{I m_T} - K\right) \tag{2.18}$$

Thereby we have set $E = E_T$, $m_1 = m_T$ and $Z_1 = z$ and introduced a correction constant K.

The specific energy loss can be given in different ways.

Stopping power The parameter $S = -\frac{dE}{dx}$ is called the stopping power for the relevant particle-target combination and has the dimension energy/length, often given in units [keV/μm], [keV/mm] or [MeV/mm], depending in which range of values the parameter lies.

Stopping cross section The parameter $\sigma = -\frac{1}{N}\frac{dE}{dx}$ is called the stopping cross section and has the dimension energy $\cdot$ area, often given in units of [eV$\cdot$cm^2] or [eV/(10^{15}atoms/cm^2)].

Total mass stopping power The parameter $\frac{1}{\rho}\frac{dE}{dx}$ is called the total mass stopping power, and has the dimension energy / (mass/area), often given in units [keV/(μg/cm^2)], [keV/(mg/cm^2)] or [MeV/(mg/cm^2)].

For the calculation of the specific energy loss, the two constants I and K are often adapted to experimental data, for example by means of SRIM-calculations [Sri08].

The used symbols are recapitulated in the following table:

For α-particles ($E_T = E_\alpha$) we obtain the following expression for the stopping cross section:

$$\sigma_\alpha = -\frac{1}{N}\frac{dE}{dx}\bigg|_\alpha = \frac{3.80}{E_\alpha[\text{MeV}]} Z \ln\left(\frac{548.58 E_\alpha[\text{MeV}]}{I[\text{eV}]} - K\right) \left[\frac{\text{eV}}{10^{15}\text{Atome}\cdot\text{cm}^{-2}}\right] \tag{2.19}$$

The mean ionization energy I and the correction constant K are to be derived from experiments (table 2).

When the material is not experimentally available, I can be calculated with the following approximation [Leo94]:

The Bethe-Bloch formula only accounts for the electron energy loss. Since the nuclear stopping increases with decreasing energy, we obtain significant deviations in the low-energy range. The stopping cross section for α-particles in aluminum is given in figure

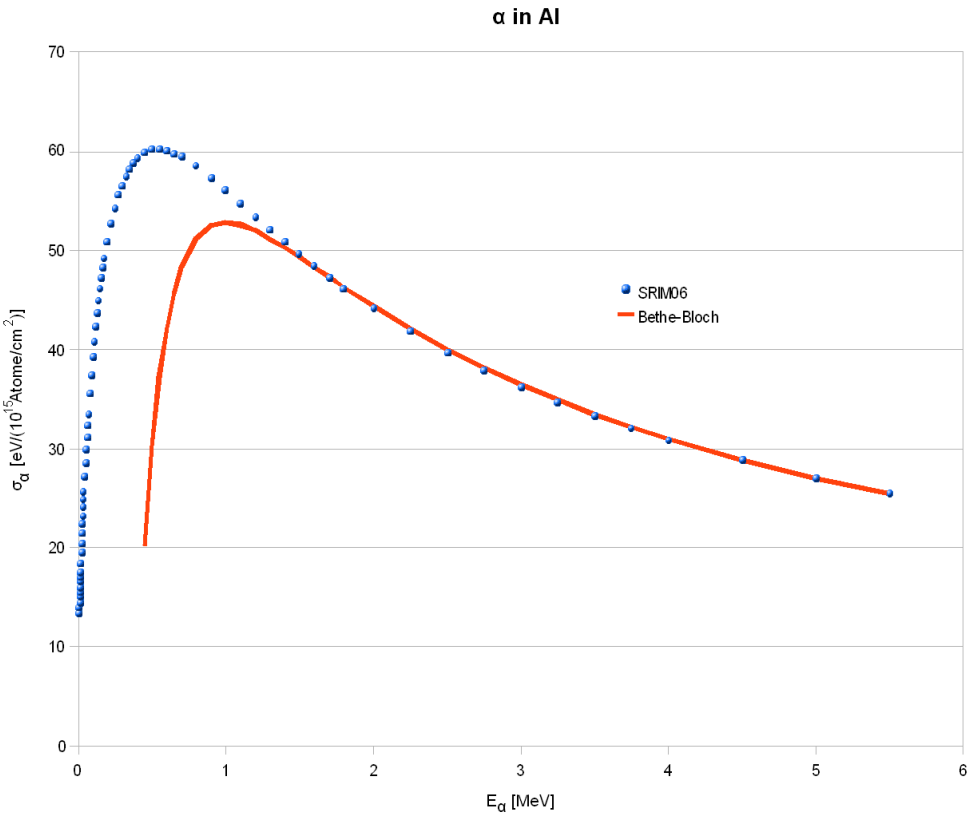

Figure 2: Stopping power of α-particles in aluminum ($I = 176.3$ [eV], $K = 0.198$) calculated using the Bethe-Bloch formula(Sektion 2.2) and with the Monte-Carlo simulation in SRIM (Appendix **??**). For $E_\alpha > 1$ [MeV] the relative uncertainty of the stopping power calculated using the Bethe-Bloch formula is smaller than 2 %.

Symbol	Parameter	Value	Unit
e	Elemental charge	$-1.602 \cdot 10^{-19}$	[As]
$m_e c^2$	Rest energy of electron	0.511	[MeV]
N_A	Avogadro constant	$6.022 \cdot 10^{+23}$	[mol^{-1}]
ε_0	Dielectric constant	$8.85 \cdot 10^{-12}$	[As/Vm]
ϵ^2	$= \frac{e^2}{4\pi\varepsilon_0}$	1.44	[eV$\cdot$ nm]
[u]	atomic unit	931.494	[MeV/c^2]
z	Ordinl number of the projectile		
m_T	Mass of the projectile		
E_T	Energy of the projectile		
Z	Ordinal number of the target atom		
I	Mean ionization energy of the target atom		
N_e	$= N \cdot Z$, Electron density of the target atom		
N	$= \frac{\rho N_A}{M}$, Particle density of the target		
ρ	Volume density of the target		
M	Molar mass of the target atoms		
K	Correction constant		

Table 1: Summary of the symbols used

Material	I [eV]	K	E_u [MeV]	rel. Uncertainty [%]
Al	176.3	0.198	1.0	2
Ar	230.6	-0.894	1.0	3
Au	1084.4	-1.064	1.5	1
C	87.1	1.039	0.8	3
Co	334.7	-0.614	1.0	2
Cu	385.3	-0.540	1.0	1
Fe	316.3	-0.649	1.0	2
Luft	95.0	0.650	0.6	1
Ne	143.7	0.544	0.8	2
Ni	360.5	-0.530	1.0	2
Ti	257.7	-0.612	1.0	2
Si	197.0	-0.507	0.6	2
H	16.05	11.80	0.6	8
O	109.0	0.332	1.0	4

Table 2: The constants I and K in the Bethe-Bloch formula for the stopping of α-particles in various materials, determined by adaption of TRIM-calculations (Appendix **??**) [Zie96]. E_u : minimal energy for the Bethe-Bloch formula with the given relative uncertainty.

2 [1]. Deviations for energies larger than 1 MeV of the Bethe-Bloch formula are smaller than 2%. Figure 4 shows the ratio of the nuclear to the electron stopping cross section as function of energy [Sri08, Zie96]. It is obvious that at high energies only the electron stopping cross section is relevant, justifying the assumptions of the Bethe-Bloch formula.

[1]The discrepancy in the Bethe-Bloch formula for low energies derives from the fact that the assumption of complete ionization of the projectile is not valid anymore!

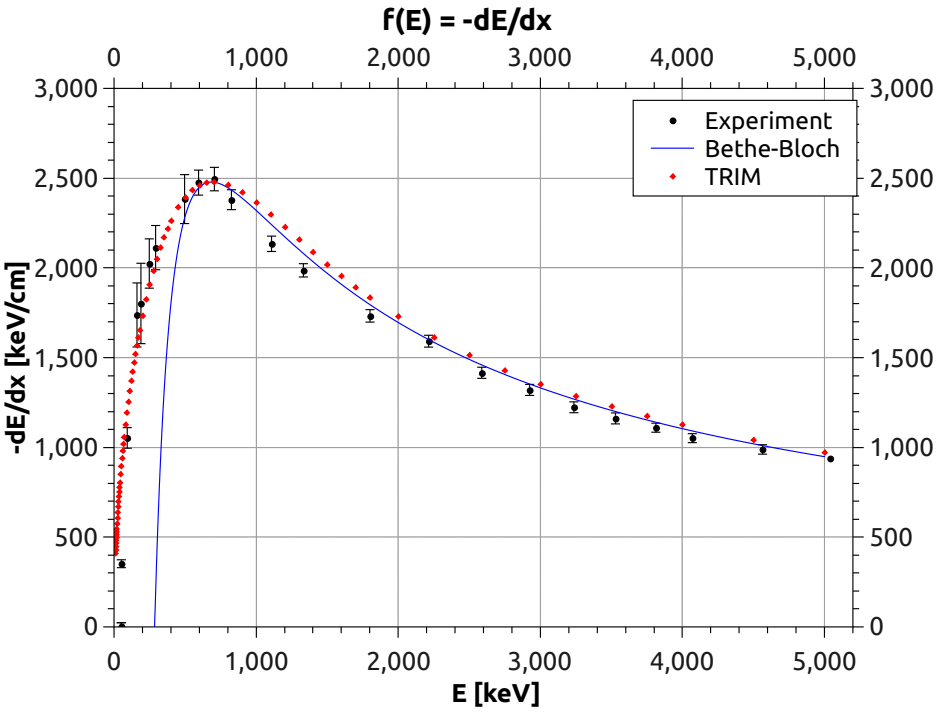

Figure 3: SRIM/TRIM in contrast to Bethe-Bloch and measurements

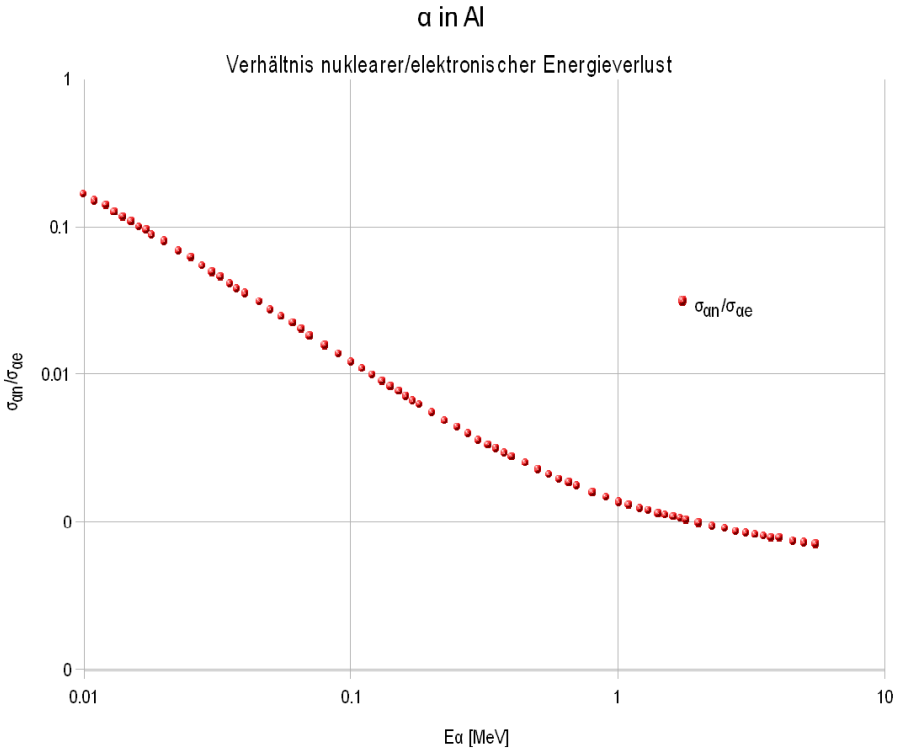

Figure 4: The ratio of the nuclear to the electron stopping power cross section for α-particles in aluminum.

2.3 Specific energy loss in compounds (Bragg's law)

The considerations so far are only valid for pure target elements.The calculations of the stopping power for compounds and mixtures require additional thought. When precise values are required one has to rely on direct measurements. However, a good estimation can often be obtained by averaging $\frac{dE}{dx}$ of the individual elements of the compound, weighted by their individual proportions. Hereby we assume that the individual contributions are independent of each other (Bragg's rule). The stopping power cross section or the total mass stopping power are best suited for this because a molecular density N is often given that is directly proportional to the density ρ of the material ($N = \frac{\rho N_A}{M}$).

For a compound $\mathrm{A}_m\mathrm{B}_n$, with m components of element A and n components of element B, the stopping power cross section $\sigma_{\mathrm{A}_m\mathrm{B}_n}$ is given by:

$$\sigma_{\mathrm{A}_m\mathrm{B}_n} = m\sigma_{\mathrm{A}} + n\sigma_{\mathrm{B}} \tag{2.20}$$

where σ_{A} and σ_{B} are the stopping powers of the atomic components A and B.

Example CO_2 $\sigma_{\mathrm{CO_2}} = \sigma_{\mathrm{C}} + 2\sigma_{\mathrm{O}}$ and $-\frac{dE}{dx}\big|_{\mathrm{CO_2}} = N_{\mathrm{CO_2}} \cdot \sigma_{\mathrm{CO_2}}$

Alternatively, we can also take the effective values for Z, M and I and directly apply equation 2.17 to calculate $\frac{dE}{dx}$.

$$Z_{\text{eff}} = \sum_i a_i Z_i, \qquad M_{\text{eff}} = \sum_i a_i M_i, \qquad \ln I_{\text{eff}} = \sum_i a_i Z_i \ln \frac{I_i}{Z_{\text{eff}}} \tag{2.21}$$

where a_i is the number of atoms of the i-th element of the molecule.

2.4 Energy straggling

2.4.1 Bohr straggling

When an energy-rich particle moves along an amorphous material, it loses energy by interaction with electrons in many individual statistically independent collisions (electron energy loss). Thus the process is biased by statistical variations.

The total number of collisions and the energy loss per collision is statistically distributed. Thus individual particles with the same starting energy E_0 will not have the same energy anymore after passing a certain layer with a thickness t. The energy ΔE is statistically distributed.

When $\Delta E \ll E_0$, then we find a normal distribution for ΔE. Therefore the probability $dW(\Delta E) = f(\Delta E)d(\Delta E)$ of finding an energy loss between ΔE and $\Delta E + d(\Delta E)$ is given by the following probability density:

$$f(\Delta E)d(\Delta E) = \frac{1}{\Omega_B\sqrt{2\pi}} \exp\left(-\frac{(\Delta E - \langle\Delta E\rangle)^2}{2\Omega_B^2}\right) d(\Delta E) \tag{2.22}$$

where Ω_B is the square root of the mean square of the deviation (standard deviation) of ΔE.

For a material with a thickness t and an electron density N_e, we thus get for $\langle \Delta E \rangle$ and Ω_B the following expressions:

$$\begin{aligned} \langle \Delta E \rangle &= E[\Delta E] = \int_{\Delta E_{min}}^{\Delta E_{max}} \Delta E f(\Delta E) d(\Delta E) \\ &= \int_{\sigma_{min}}^{\sigma_{max}} \Delta E dW = N_e t \int_{\sigma_{min}}^{\sigma_{max}} \Delta E d\sigma \end{aligned} \tag{2.23}$$

and:

$$\Omega_B^2 = Var[\Delta E] = E[\Delta E^2] - (\langle \Delta E \rangle)^2 \simeq E[\Delta E^2] = N_e t \int_{\sigma_{min}}^{\sigma_{max}} \Delta E^2 d\sigma \tag{2.24}$$

With:

$$d\sigma = \frac{d\sigma/db}{d(\Delta E)/db} d(\Delta E), \qquad \Delta E = \frac{c}{b^2}, \qquad c = \frac{Z_1^2 Z_2^2 \epsilon^4}{E_0} \frac{m_1}{m_2} \tag{2.25}$$

we obtain:

$$d\sigma = -\pi \frac{c}{\Delta E^2} d(\Delta E) \tag{2.26}$$

and therefore:

$$\Omega_B^2 = \pi c N_e t \int_{\Delta E_{min}}^{\Delta E_{max}} d(\Delta E) = \pi c N_e t (\Delta E_{max} - \Delta E_{min}) \tag{2.27}$$

With $N_e = NZ$, $Z_2 = 1$, $m_2 = m$, ΔE_{max} from equation 2.9 and $\Delta E_{min} = I$, we obtain:

$$\Omega_B^2 \simeq 4\pi Z_1^2 \epsilon^4 NZt \left(\frac{m_1}{m_1 + m} \right)^2 \simeq 4\pi Z_1^2 \epsilon^4 NZt \tag{2.28}$$

because $m \ll m_1$.

Ω_B is called Bohr straggling because it was first derived by Bohr. The equation 2.28 is only valid for small layer thicknesses t.

The Bohr theory tells us that the energy straggling is not dependent on the energy of the projectile and is proportional to the square root of the electron density per unit area.

The full line broadening Γ (full width at half maximum, FWHM) of the energy distribution that is caused by the straggling, is therefore:

$$\Gamma = 2\sqrt{2 \ln 2}\Omega \simeq 2.355\Omega \tag{2.29}$$

where Γ generally stands for energy straggling, independent of the theory.

The line width Γ_{exp} of the peak, that is measured in the experiment derives from the finite thickness of the source Γ_Q and the detector resolution Γ_D, which is also normally distributed. Because their parts are statistically independent, we obtain the following for Γ:

$$\Gamma = \sqrt{\Gamma_{exp}^2 - \Gamma_Q^2 - \Gamma_D^2} = \sqrt{\Gamma_{exp}^2 - \Gamma_0^2} \tag{2.30}$$

We therefore find that for the energy distribution of the α-particles:

$$N(E) = \frac{N_0}{\Omega\sqrt{2\pi}} \exp\left(-\frac{[E - (E_0 - \langle \Delta E_0 \rangle)]^2}{2\Omega_B^2}\right) \tag{2.31}$$

where N_0 is the total number of particles in the peak, $N(E)$ the number of α-particles with an energy in the interval $[E, E + dE]$, and E_0 is the energy before the interaction.

However, equation 2.31 is only valid for small layer thicknesses t. Other influences have to be considered for larger thicknesses.

2.4.2 Anomalous energy straggling

When the energy distribution of the α-particles has a certain width from the beginning, another effect shows up that is of no statistical origin but can be attributed to the fact that the specific energy loss is dependent on the energy of the particles [Pri82].

The specific energy loss (stopping power S) has a maximum that lies in the energy range between 0.5 and 1 [MeV] for α-particles.

S rises monotonously with decreasing energy in the range above the maximum. The particles therefore lose less energy on the high-energy side! This fact leads to an increased peak width, independent of the widening caused by the Bohr straggling. In the energy range below the maximum, S decreases again and thus the particles rapidly lose less energy again. This, on the contrary, leads to a narrowing of the energy distribution.

2.5 Range and range straggling

The range R of particles with an initial energy E_0 entering a material is an important parameter that is relatively simple to access. It is also possible to access the initial energy when the range is known. Furthermore, the knowledge of the stopping is important to dimension detectors used in radiotherapy and ion implantation as an important technique to dope semiconductors.

2.5.1 Theoretical consideration

The range can principally be calculated simply by integration when the specific energy loss as function of the particle energy is known:

$$R(E_0) = \int_0^{E_0} \left(\frac{dE}{dx}\right)^{-1} dE \tag{2.32}$$

The result is the total range what can be visualized either in a nuclear-track emulsion or a bubble nebula chamber. Here, it is visible, that the probability for a nuclear scatter and thereby larger angular scattering strongly increases towards the end of the stopping range. Still, the tracks are relatively straight for heavy particles as, for example, the α-particles and thus the range is also relatively sharp. We just get for the reason of the

statistical process of the stopping power a mean range R_m with a range straggling Ω_R bzw. $\Gamma_R = 2.355\Omega_R$. The energy-range-relationship is also important because for a known particle, the initial energy can be determined with a measured range.

In practice, a semi-empirical formula is used:

$$R(E_0) = R(E_{min}) + \int_{E_{min}}^{E_0} \left(\frac{dE}{dx}\right)^{-1} dE \tag{2.33}$$

where E_{min} is the minimal energy for which the $\frac{dE}{dx}$-formula (Equation 2.17) is valid. $R(E_{min})$ is a constant that is experimentally determined.

Some principles, derived from equation above, are given as follows:

Energy dependency The strong energy dependency of $\frac{dE}{dx}$ (see equation 2.17) is expressed in the first term in the form of $\frac{a}{E}$ (a is a constant). The second term with $\ln \frac{E}{b}$ shows only a week energy dependence (b is a constant). Setting the second term constant, we obtain a dependency for the range in form of:

$$R \propto E_0^2 \tag{2.34}$$

The logarithmic term results in a reduction of the exponent. The range is therefore approximately proportional to $E_0^{3/2}$

This empirical law originates from Geiger and is precise to approximately 10% in the range of 4 to 10 [MeV]. A better appoximation for the mean range is given by:

$$R(E) = a_2 E^2 + a_1 E + a_0 \tag{2.35}$$

The constants a_i are experimentally determined. Table 3 gives the constants for the different materials used in the experiment (determination of foil thickness).

Material	a_2 [μm/MeV^2]	a_1 [μm/MeV]	a_0 [μm]	rel. Uncertainty [%]
Al	0.3796	2.2550	0.7002	3
Au	0.1025	1.1145	0.2868	3
Co	0.1466	1.0032	0.4346	2
Cu	0.1420	1.1939	0.5765	3
Fe	0.1599	1.0628	0.4341	2
Ni	0.1379	1.0727	0.4793	4
Si	0.4231	2.6021	0.5253	5
Ti	0.2782	1.5665	0.4900	2
Mumetall	0.1423	1.0809	0.4670	2
Mylar	0.5894	2.2398	1.1487	1

Table 3: Constants a_i for the foils used in the experimental part. In the last column the relative uncertainty of the polynomial formula to the TRIM-calculation is given for the range of 0.6 and 10 [MeV].

Furthermore the following useful rules can be obtained: $R \propto (m_T Z)^{-2}$ for different particles (mass $m_{T,i}$, charge Z_i) with the same energy E_T in the same media

$$R(E_T, m_{T,1}, Z_1) = \left(\frac{m_T 2 Z_2}{m_{T,1} Z_1}\right)^2 R(E_T, m_{T,2}, Z_2) \tag{2.36}$$

This allows one to derive the energy-range-relationship from the α-particles for protons, deuteron etc.

The stopping power $S = \frac{dE}{dx}$ is proportional to the electron density N_e in relation to the absorption material.

$$N_e = NZ = \frac{N_A Z}{M}\rho \tag{2.37}$$

The ratio $\frac{Z}{M}$ is approximately equal for all elements (with the exception of heavy ions and hydrogen):

$$\frac{N_e}{\rho} = \frac{NZ}{\rho} \simeq \text{const} \tag{2.38}$$

It therefore makes sense to give the layer thickness and the range in units of mass per area (e.g. in [mg/cm^2]) instead of in units of charge (e.g. [cm]):

$$d\xi = \rho dx, \qquad \frac{dE}{d\xi} = \frac{dE}{d(\rho x)} = \frac{1}{\rho}\frac{dE}{dx} \tag{2.39}$$

Bragg-Kleemann-rule For the same particle in different materials with density ρ_i and molar mass M_i the following rough approximation can be given:

$$\frac{R_1}{R_2} \simeq \frac{\rho_2}{\rho_1}\sqrt{\frac{M_1}{M_2}} \tag{2.40}$$

Range in compounds The following rough approximation can be given for the range R_{comp} in compounds:

$$R_{comp} = \frac{M_{comp}}{\sum_i \frac{a_i M_i}{R_i}} \tag{2.41}$$

where: M_{comp} is the molar mass of the compound, M_i and R_i are the molar mass and the range, respectively, in the individual compound i, and a_i is the relative number of atoms in the compound i.

2.5.2 Determination of ranges

The range and range straggling of α-particles in a gas (in this experiment air) can be determined measuring the so-called number-distance curve. The number-distance curve depicts the count rate of α-particles as a funcion of the distance x between the source and the detector. Notice that the geometry of the apparatus is changed when varying the distance, i.e. the solid angle captured by the detector increases for decreasing x. (Alternatively, the measure can be done with a constant x but instead decreasing pressure in the chamber which leads to a decreasing effective layer thikness.)
To do the measurement, the vakuum chamber is filled with air and the distance x between source and detector is increased to the point where no α-particle reaches the detector anymore. The distance is now reduced step by step, making a measurement

of a few minutes for each position.
The range spectrum is in a first order approximation described by a Gaussian distribution:

$$n(R) = \frac{1}{\sqrt{2\pi\Omega_{\mathrm{R}}^2}} \exp\left(-\frac{(R_m - R)^2}{(2\Omega_{\mathrm{R}})^2}\right) \tag{2.42}$$

with mean range R_m (center of the distribution $n(R)$),
range straggling Ω_{R} and therefore $\Gamma_{\mathrm{R}} = 2.355\Omega_{\mathrm{R}}$ = Full With at Half Maximum.
What is actually measured is the fraction of α-particles, which are not yet stopped after penetrating the layer x. This fraction is given by:

$$\begin{aligned}\tilde{n}(x) &= 1 - \int_{-\infty}^{x} n(R')\,\mathrm{d}R' \\ &= 1 - \int_{-\infty}^{x} \frac{1}{\sqrt{2\pi\Omega_{\mathrm{R}}^2}} \exp\left(-\frac{(R_m - R')^2}{(2\Omega_{\mathrm{R}})^2}\right)\,\mathrm{d}R'\end{aligned} \tag{2.43}$$

Vice versa, the distribution $n(R)$ can be found by differentiating the measured curve $\tilde{n}(x)$. Both distributions are shown in Fig. 5.

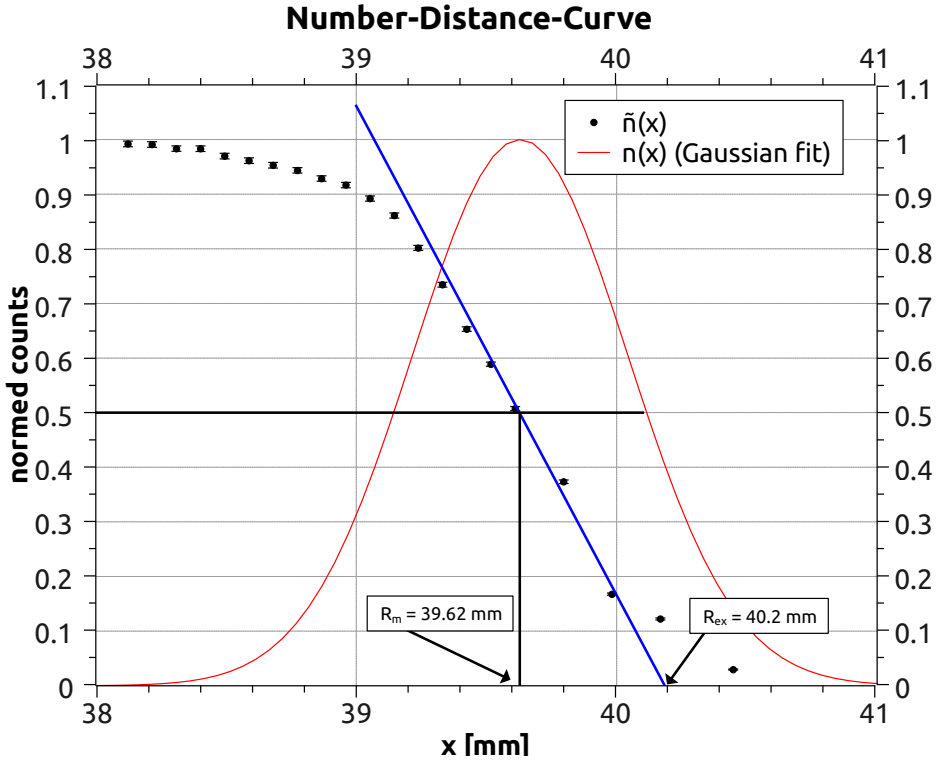

Figure 5: Normalized number-distance curve for α-particles from a ^{241}Am source in air, and the corresponding interpolated range spectrum.
R_m: mean range, R_{ex}: extrapolated range

The relation between the parameters R_m, R_{ex} and the measured straggling Ω_{RM} is

given by

$$\frac{R_{\text{ex}} - R_m}{1/2} = \sqrt{2\pi} \cdot \Omega_{\text{RM}} \tag{2.44}$$

which leads to the value of the measured FWHM:

$$\Gamma_{\text{RM}} = 2.355 \cdot \Omega_{\text{RM}} = 2.355 \frac{2}{\sqrt{2\pi}} (R_{\text{ex}} - R_m) \tag{2.45}$$

To finally find the true range straggling Γ_{R}, the term has to be corrected by

$$\Gamma_{\text{R}} = \sqrt{\Gamma_{\text{RM}}^2 - \Gamma_0^2} \tag{2.46}$$

where Γ_0 is the range straggling at $0\,\text{mbar}$. The cause of this term is the fact that the α-particles do have a finite spectral linewidth. The value Γ_0 can be found by extrapolating the measured curve $\Gamma_{\text{RM}}(p)$ for $p \to 0$.

2.5.3 Residual Range

The experimentally determined data for the range of the α-particles produces too small values. The reason for this is that there is an energy threshold E_S in the experiments, under which no α-particles are detectet (see spectrum in fig. 6).

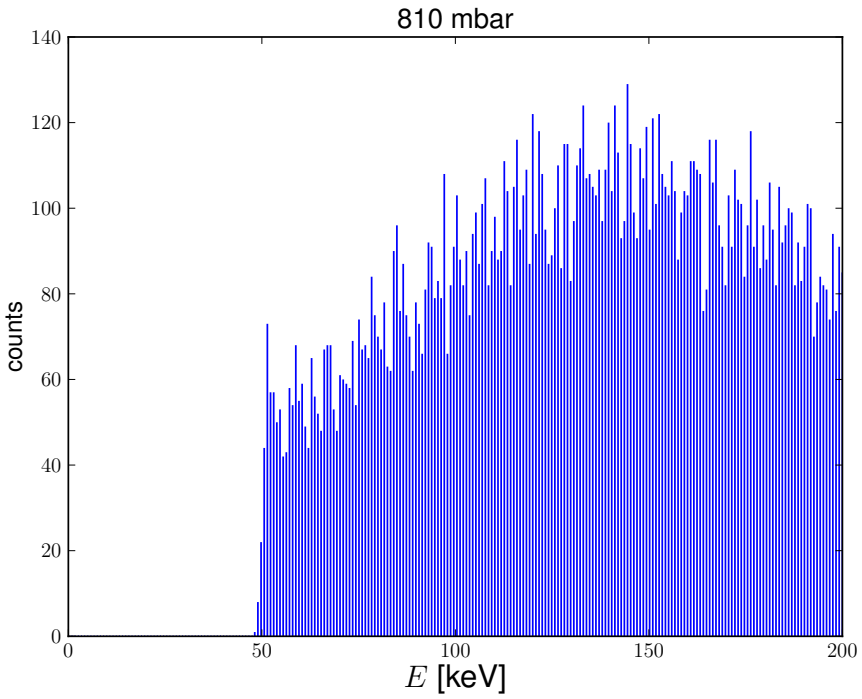

Figure 6: Energy threshold in a energy spectrum plot

The so-called residual range $R(E_S) = R_S$, which has to be added to the measured values, can be found by using equation (2.47).

In the experiment, the energy E and the stopping power $\mathrm{d}E/\mathrm{d}x$ are determined. It becomes apparent that the ratio $E/(\mathrm{d}E/\mathrm{d}x)$ barely changes over a great range of energy. It turns out that the residual range can be approximated by:

$$R_S = \frac{3}{2} \frac{E_S}{-(\mathrm{d}E/\mathrm{d}x)_S} \tag{2.47}$$

It is important to notice that it is not an easy task to estimate the denominator of this term. It might be an option to also do a TRIM-simulation to find a reasonable estimate.

2.6 Energy loss in foils (absorber)

The energy loss ΔE that a charged particle with an energy E_0 loses by passing through a thin absorber with thickness t, can be approximated by following equation:

$$\Delta E = \left(\frac{dE}{dx}\right)_m t \tag{2.48}$$

where $\left(\frac{dE}{dx}\right)_m$ is the stopping power averaged over the energy of the particle in the range E_0 and $E_0 - \Delta E$. The value E_0 can be taken when the energy loss is small and thus the stopping power hardly changes.

For a thicker absorber that causes a strong energy loss, we have to follow a different way:

- One possibility is to divide the absorber into many thin layers with a thickness t_i:

  $$t = \sum_{i=1}^{n} t_i \tag{2.49}$$

  The individual energy loss ΔE_i in the thin layers at an energy $E_{i-1} - \Delta E_i$ has then to be calculated step by step and summed up to obtain the total energy loss:

  $$\Delta E = \sum_{i=1}^{n} \Delta E_i \tag{2.50}$$

  The number of layers n has to be so large, that the stopping power in a single layer can be taken as constant.

- A simpler possibility exists when the energy-range relationship is known for the particle-absorber combination, see figure 7 [Kno00].

  R_0 is the range of the particle with an energy E_0. We then obtain the range R_t by subtracting the foil thickness t from R_0. R_t is exactly the stopping range, that a particle with the energy E_t would have in the material of the foil. Therefore we determine E_0 and E_t and then take the values R_0 and R_t from the energy-range curve to determine the foil thickness from the difference:

  $$\Delta E = E_0 - E_t, \qquad t = R_0 - R_t \tag{2.51}$$

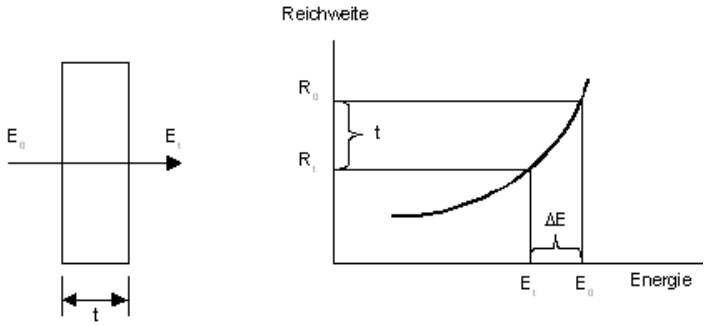

Figure 7: An illustration of the determination of the foil thickness from the energy-range relationship. E_0 : entrance energy, E_t : exit energy, $\Delta E = E_0 - E_t$ (energy loss in the foil), R_0 : range for E_0, R_t : range for E_t, $t = R_0 - R_t$ (foil thickness).

3 Measurement setup

3.1 Overview of the apparatus

The setup of the used apparatus is given in figure 8. The α-source (^{241}Am) and the detector are aligned on an axis in a glass cylinder (vacuum-tight chamber). 7 scatter foils made from different materials on a wheel can be put into the fixed distance between detector and source. The chamber can be pumped down to about 0.5 [mbar]. The detector signals are processed outside the box and fed via a multi-channel analyzer (ADC) card into a PC.

Figure 8 shows the setup for gas. The only difference to the setup for solids is the variable distance of the source to the detector instead of the absorption foil.

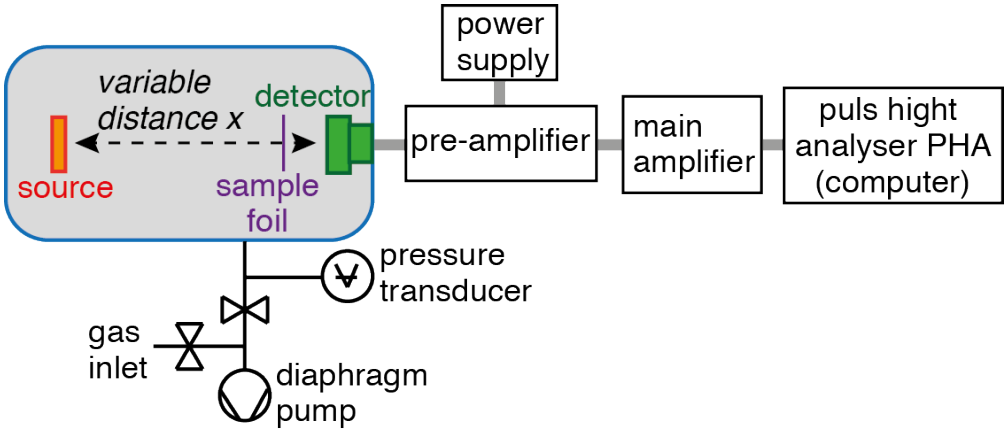

Figure 8: Experimental setup for the determination of the absorption of α-particles in gas.

3.2 Components of the apparatus

3.2.1 Diaphragm pump

A diaphragm pump is a positive displacement pump that uses a combination of the reciprocating action of a rubber, thermoplastic or teflon diaphragm and suitable non-return check valves to pump. The diaphragm pump evacuates completely oil-free (no oil vapors). The oil pump of the type N 813.4 ANE (Neuberger) used in this experiment has two stages and reaches a final pressure of 0.5 hPa with a pumping speed of 13 l/min.

3.2.2 Source

The α-source is ^{241}Am plated in an area with a diameter of 7 [mm] on a metal disc. The ^{241}Am has a half-life of 432 [y] and therefore the activity (I_S (1.5 [μCi] = 185 [kBq]) can be assumed to be constant over the course of the experiment). α-particles with different energies are emitted (4 groups of particles can be resolved, see appendix A).

3.2.3 Sample foils

Different sample foils mounted on a wheel (positions 2 to 8) can be rotated in between the detector and source (7 [mm] from the detector). Position 1 is empty. The information about the allocation of the foils and their properties can be found in appendix C.

3.2.4 Variable distance

The position of the source can be adjusted with respect to the detector and the sample foil. By varying the distance for different measurements with a fixed gas pressure, one can gather data for different effective layer thicknesses.

3.2.5 Detector

A surface barrier detector is used to detect the α-particles (see figure 9). It is p-doted single crystalline silicon coated with a thin aluminum layer. The specific resistance of the silicon is 3800 [Ωcm]. When applying a voltage of -100 [V], the detector has a sensitive layer of at least 100 [μm] [Leo94], which is enough to stop α-particles with an energy of more than 10 [MeV] (see figure 10). The α-particles produce a charge pulse with an amplitude Q_I, that is proportional to the energy deposited in the sensitive layer. The active surface of the detector is 50 [mm^2]. The energy resolution of the detector is about 18 [keV] for 5.5 [MeV] for α-particles.

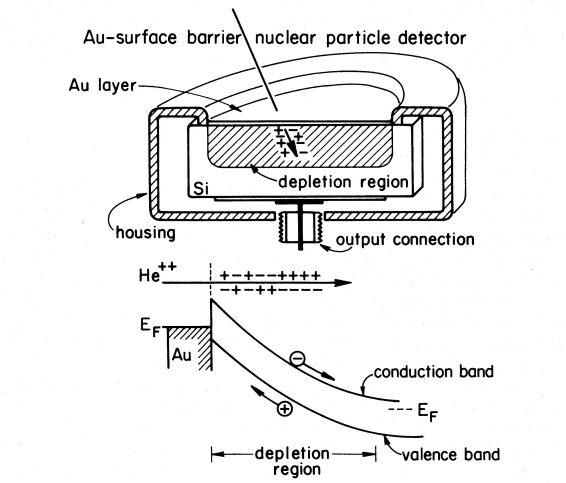

Figure 2.3 Schematic diagram of the operation of a gold surface barrier nuclear particle detector. The upper portion of the figure shows a cutaway sketch of the silicon disc with gold film mounted in the detector housing. The lower portion shows an alpha particle, He^{++} ion, forming holes and electrons over its penetration path. The energy band diagram of a reverse biased detector (positive polarity on *n*-type silicon) shows the electrons and holes swept apart by the high electric field within the depletion region.

Figure 9: Schematic presentation of a surface barrier detector [Fed86].

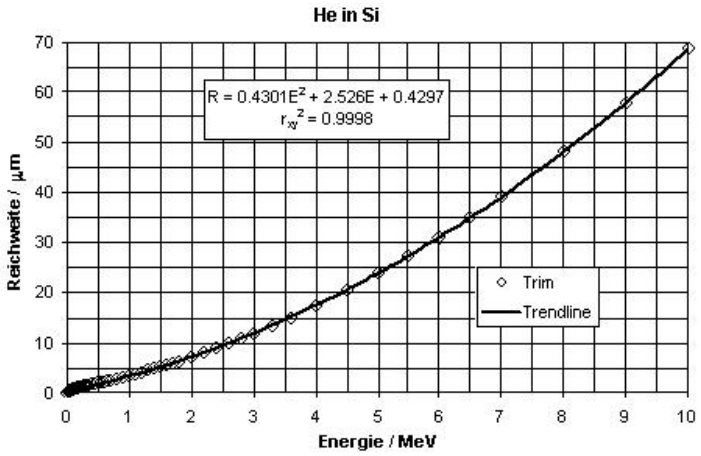

Figure 10: Energy-range curve for α-particles in silicon [Sri08].

3.2.6 Electronics

The pre-amplifyer positioned close to the detector outside the chamber converts the charge pulse Q_I from the detector into a voltage pulse Q_I, and is therefore also proportional to the particle energy. The main amplifier is then responsible for the final signal amplification and shaping of the signal, so that it can be converted to a digital value with a multichannel analyzer.

3.2.7 Computer

Measurement program: Setup as pulse height analyzer (PHA), setting the amplification to 8182 channels.

You can switch between the measurement program and other programs without stopping data acquisition!

3.2.8 Detector voltage and amplification

Have a look at the pulse shape of the detector signals after the per-amplifier. Switch the main amplifier to the right polarity (MCA needs positive pulses, between 0 and +10 V). Set the amplification gain for the 5.5 MeV α-particles to get about 9 V signals (use oscilloscope). Don't change the gain over the course of the measurement again!

4 Safety instructions

It is strictly required that you read all safety instructions given in appendix E, which are also displayed at the testing site!

4.1 Start-up of the experiment

- Computer

  Start-up computer.

  Open program for acquisition and analysis of spectra $Start > Programme > FA8T > MCA - 3$

  Open program for the control of the wheels with the foils $Start > Programme > Stepper$

- Detector voltage

  Ensure that the chamber (glass cylinder) is totally covered with the light-shield. The detector is light-sensitive!

  Detector voltage must be set to zero before the power supply is switched on!

  The detector voltage must be increased slowly until -100 [V] is reached. Max. voltage: -120 [V], check current!

  Never remove the light-shield from the chamber when there is still a voltage on the detector!

- Evacuation of the chamber

  Close the valve to the chamber (V1, see figure **??**) and the venting valve (V2).

  Switch on the vacuum pump and pump down the tube first. Then open the V1 slowly (otherwise foils may brake!) and pump down the chamber (within 3-5 minutes). On the oscilloscope you can now see the α-particles entering the detector.

- Electronics

  Switch on the amplifier right at the beginning (while the electronics heat up, shifts in the detector signals may be observed).

4.2 End of experiment

- Detector voltage

  The detector voltage has to be set to zero slowly, before the power supply is switched off.

- Venting of the chamber

  Switch off pump. Open V2 valve. Open V1 valve very slowly to vent the chamber with about 2 [mbar/s] (otherwise foils may brake!).

  Move two thick foils between the source and detector. No α-particles should reach the detector anymore.

- Oscilloscope (if existing)
  Switch off.
- Electronics
  Switch off.
- Computer
  Close programs and switch off.

5 Experimental tasks

Test sites 1 and 2

The stopping power of α-particles in gas shall be examined in the following experiment. Firstly, the specific energy loss and the energy straggling of the α-particles will be studied in detail. Secondly, the thickness of thin foils of known composition will be determined.

5.1 Preparation for the experiment

5.1.1 Kinetic energy of the α-particles

Calculate the kinetic energy T_i of the α-particles, that are emitted by an ^{241}Am-source (see appendix B).

Following this, determine the mean energy T_m by using the relative probablities for the transitions.

5.1.2 Specific energy loss

Calculate with the Bethe-Bloch formula (section 2.2) the stopping power of α-particles in air (Bragg's law, see section 2.3) in units [eV/(10^{15} atoms/cm^2)] and [keV/mm].

5.2 Alpha spectra of Am-source and calibration of the detector

Acquire the energy distribution of the α-particles when the chamber is evacuated. Determine the mean energy of the individual transitions and their relative frequency. Use the results to calibrate together with section 5.1.1 the detector (one-point calibration).

Make sure that there isn't any foil between the source and the detector!

Determine:

Peak position	E_i
Peak width	Γ_i
Peak heigth	N_i (average over several channels)
Peak volume	$N_i\Gamma_i$
Abundance	$H_i = \frac{N_i\Gamma_i}{\sum_{i=1}^{4} N_i\Gamma_i}$

5.3 Foil thickness

Determine the thickness of the sample foils by using the measured energy loss of the α-particles.

Calculate the foil thickness with both the Bethe-Bloch formula and polynomial formulae using experimental values (table 3 in chapter 2.5). Compare both results.

5.4 Energy distribution / stopping range

Determine the number-distance curve and use it to find the stogging range, i.e. the mean and extrapolated distance R_m and R_{ex}. Also find the range straggling Γ_R.
Find the residual range R_S and reconsider the distances measured.
Compare your results to those in literature.

Use STP (standard conditions for temperature and pressure) for ranges. ($273.15\,\mathrm{K}$, $101.325\,\mathrm{kPa}$)

5.5 Specific energy loss

Determine the energy distribution of the α-particles as a function of gas pressure p $\Rightarrow E = E(p)$, $\Gamma_E = \Gamma_E(p)$ (E: mean energy, Γ_E: full width half maximum). Use the effective layer thickness $x = x_0 \frac{p}{p_0} \frac{T_0}{T}$ with STP $p_0 = 1013.25$ hPa and $T_0 = 273.15$ K) for your computations.
Then determine:

- The specific energy loss $-\frac{dE}{dx} = f(x)$
- The values of x_{max}, E_{max} and $-\frac{dE}{dx}_{max}$ for the maximal specific energy loss
- The specific energy loss as a function of the energy of the particle (Bragg curve) and compare with the theory (Bohr straggling)
- Compare the measured energy straggling $\Gamma = f(x)$ with the theory (Bohr straggling). (don't forget to correct the measured energy width according to equation 2.30 (no foil: $\Gamma_{exp}(0)^2 = \Gamma_Q^2 + \Gamma_D^2$).

5.6 Discussion

Compare and discuss in detail the experimental results with the theoretical predictions.

Appendix

A Stopping Range of the α-decay

The source for the α-particles is ^{241}Am (Americium) plated on a metal disc (thin layer). ^{241}Am α-decays with a half-life of n 432 [y]:

$$^{241}\text{Am} \longrightarrow {}^{237}\text{Np}^* + \alpha$$

The remaining element is ^{237}Np (Neptunium), likely in an excited state with an excitation energy of E_Ex. This energy is most often emitted as electro-magnetic radiation. The kinetic energy T of the emitted α-particles can be calculated based on the conservation of energy and momentum. We can assume an infinite thin source with no self-absorbtion of energy.

The energy balance of the α-decay of ^{241}Am is given as a diagram in figure 11. The total energy is conserved. We can therefore establish the following equation for the energy balance:

$$\begin{aligned} m(^{241}\text{Am})c^2 &= [m^*(^{237}\text{Np}) + m(^4\text{He})]c^2 + T \\ &= [m(^{237}\text{Np}) + m(^4\text{He})]c^2 + T + E_Ex \end{aligned} \tag{A.1}$$

$$Q_0 = [m(^{241}\text{Am}) - m(^{237}\text{Np}) - m(^4\text{He})]c^2 \tag{A.2}$$

where $m^*(\text{X})c^2 = m(\text{X})c^2 + E_Ex$ is the rest energy of the excited nucleus X. Q_0 is the decay energy and is the maximum value for the kinetic energy T, that is available. The mass of the neutral atoms have to be applied (appendix B).

It can be written simply as: $m(^{241}\text{Am}) = m_{\text{Am}}$, etc.

$$T = Q_0 - E_Ex = T_\alpha + T_{\text{Np}} \tag{A.3}$$

Different groups of α-particles with discrete energies $T_{\alpha,i}$ are emitted, based on the discrete vales $E_{A,i}$ of the excitation energy of the remaining nucleus.

$$T_i = Q_i = Q_0 - E_{A,i} = T_{\alpha,i} + T_{\text{Np},i} \tag{A.4}$$

The kinetic energy T_i is shared by the α-particle and the remaining nucleus.

Momentum balance Because a resting ^{241}Am-nucleus decays, we obtain:

$$\vec{0} = \vec{p}_\alpha + \vec{p}_{\text{Np}} \tag{A.5}$$

which means:

$$p_\alpha^2 = p_{\text{Np}}^2, \qquad T_{\text{Np}} = T_\alpha \frac{m_\alpha}{m_{\text{Np}}} \tag{A.6}$$

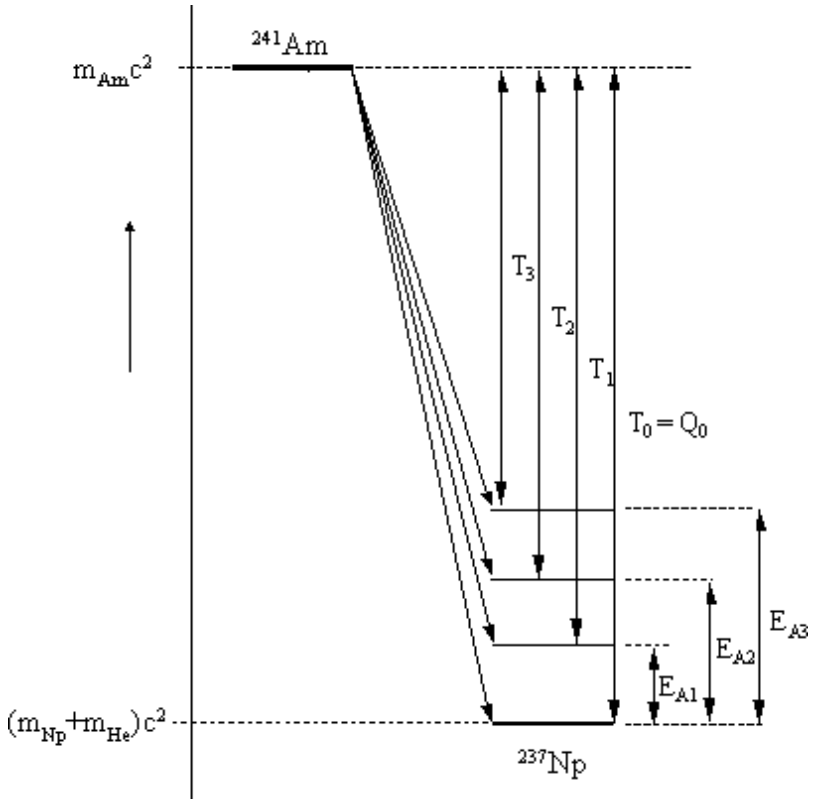

Figure 11: Energy balance of the α-decay of ^{241}Am.

and therefore:

$$T_{\alpha,i} = \frac{Q_i}{1 + m_\alpha/m_{\mathrm{Np}}} = \frac{Q_0 - E_{A,i}}{1 + m_\alpha/m_{\mathrm{Np}}} \tag{A.7}$$

The intensity $I_{\alpha,i}$ of the most intense α-particle groups are given in table 4. Calculate the energy $T_{\alpha,i}$ of the α-particles by means of the given values of the excitation energies $E_{A,i}$. The required values for the masses in atomic units are given in appendix B.

i	$E_{A,i}$ [keV]	$I_{\alpha i}$ [%]
0	0	0.34
1	33.2	0.22
2	59.54	84.5
3	102.96	13.0
4	158.51	1.6

Table 4: Excitation energies and transition probabilities for the α-decay of ^{241}Am in ^{237}Np.

B Atomic mass for the calculation of the energy of the α-particles

Quelle: Nucl. Phys. A595 (1995) 409-480

$$
\begin{aligned}
m(\alpha) &= 4.001487900 \text{ [u]} \\
m(^4\text{He}) &= 4.002603250 \text{ [u]} \\
m(^{237}\text{Np}) &= 237.048167253 \text{ [u]} \\
m(^{241}\text{Am}) &= 241.056822944 \text{ [u]} \\
1 \text{ [u]} \cdot c^2 &= 931.49432 \text{ [MeV]}
\end{aligned}
$$

The excitation energy of the ^{237}Np-nucleus and the transition probability (respectively the abundance) can be found in the book at the test site [Led67].

C Sample foils

Foils Test site 1 Position	Material	Z	r [$\frac{g}{cm^3}$]	N [$10^{22} At./cm^3$]
1	$\emptyset$	-	-	-
2	Al	13	2.70	6.03
3	Al	13	2.70	6.03
4	Ti	22	4.52	5.68
5	Fe	26	7.87	8.48
6	Ni	28	8.90	9.13
7	Au	79	19.32	5.91
8	Mumetall		8.81	8.83

Table 5: Position and properties of the absorption foils of test site 1

Foils Test site 2 Position	Material	Z	r [$\frac{g}{cm^3}$]	N [$10^{22} At./cm^3$]
1	$\emptyset$	-	-	-
2	Al	13	2.70	6.03
3	Al	13	2.70	6.03
4	Cu	29	8.92	8.45
5	Co	27	8.90	9.09
6	$\emptyset$	-	-	-
7	Au	79	19.32	5.91
8	Mylar		1.40	9.63

Table 6: Position and properties of the absorption foils of test site 2

	Atom	Z	Atom-%
Mylar	H	1	36.36
	C	6	45.45
	O	8	18.18
Mumetall	Ni	28	77.0
	Fe	26	14.0
	Cu	29	5.0
	Mo	42	4.0

Table 7: Properties of Mylar and Mumetall

D Lab protocol

Proposition for the layout of the lab protocol. The following points should be included:

1. Name/title of the experiment
2. Username and date
3. Abstract
4. Conceptual formulation
5. Short introduction

   Theoretical basics, most important formulae with their extent of validity etc.
6. Measurement method
7. Experimental setup

   Used instruments, block diagram
8. Measurement results (table with results in the appendix)
9. Evaluation of the results
   - Figure with experimentally derived data with error bars.
   - Summary of the measurement results
10. Discussion of the results
11. Bibliographical reference

Note to the content of the "Abstracts" The purpose of the abstract is to give readers concise information about the content of the article. The abstract should be informative and not only indicate the general scope of the article but also state the main results obtained and conclusions drawn. The abstract is not part of the text and should be complete in itself; no table numbers, figure numbers, references or displayed mathematical expressions should be included. It should be suitable for direct inclusion in abstracting journals and should not normally exceed 200 words. If the article is not in English, an English version of the abstract must also be supplied. Since contemporary information-retrieval systems rely heavily on the content of titles and abstracts to identify relevant articles in literature searches, great care should be taken in constructing both. Some authors find difficulty in abstracting their own articles and it is therefore suggested that they seek the help of a colleague when in doubt. (From: Institute of Physics / Notes for Authors)

E Safety instruction for the Alphaabsorption experiment

The vacuum chamber must never be opened. The activity of the ^{241}Am-source has an activity of 1.5 [μCi] = 185 [kBq]. More information about radioactivity and radiation protection can be found in [Vol07].

Additionally, the measurement setup contains some expensive and sensitive components (pressure transducer, detector, foils, amplifiers), that can easily be destroyed, when for example the pressure or the detector voltage is changed quickly! Please consider the following instructions to avoid any damage!

- Detector voltage

  The detector voltage has to be set to zero slowly before the power supply is switched off.

- Venting of the chamber

  Switch off pump. Open V2 valve. Open V1 valve very slowly to vent the chamber with about 2 [mbar/s] (otherwise foils may brake!).

  Move two thick foils between the source and detector. Now, no α-particles should reach the detector anymore.

- Electronics

  Properly switch off all electronic instruments!

References

[Boh13] N. Bohr, Phil. Mag. **25** (1913) 10. 6

[Fed86] L.C. Feldman and J.W. Mayer *Fundamentals of surface and thin film analysis*, New York, 1986. 23

[Kno00] G.N. Knoll, *Radiation Detection and Measurement*, Third Edition, John Wiley & Sons Inc., New York, 2000. 20

[Led67] C. Lederer, M. Hollander and J.M.I. Perlman, *Table of Isotopes*, John Wiley & Sons Inc., Sixth Edition, London, 1967. 31

[Leo94] W.R. Leo, *Techniques for Nuclear and Particle Physics Experiments*, Second Revised Revision, Springer-Verlag, Berlin, 1994. 9, 23

[Ous78] P. J. Ouseph and A. Mostovych, Am. J. Phys. **46** (1978) 742.

[Pri82] R. M. Prior and A.A. Rollefson, Am. J. Phys. **50** (1982) 457. 15

[Sri08] Srim 2008, http://www.srim.org 9, 11, 24

[Vol07] M. Volkmer, *Radioaktivit‰t und Strahlenschutz*, Informationskreis KernEnergie, Berlin, 2007. In PDF-Format : http://www.kernenergie.de/r2/documentpool/de/Gut_zu_wissen/Materialen/Downloads/013radioaktivitaet_strahlenschutz2007.pdf 34

[Zie96] J.F. Ziegler, J.P. Biersack and U. Littmark, *The Stopping and Range of Ions in Solids*, Pergamon Press, New York, 1996. 11